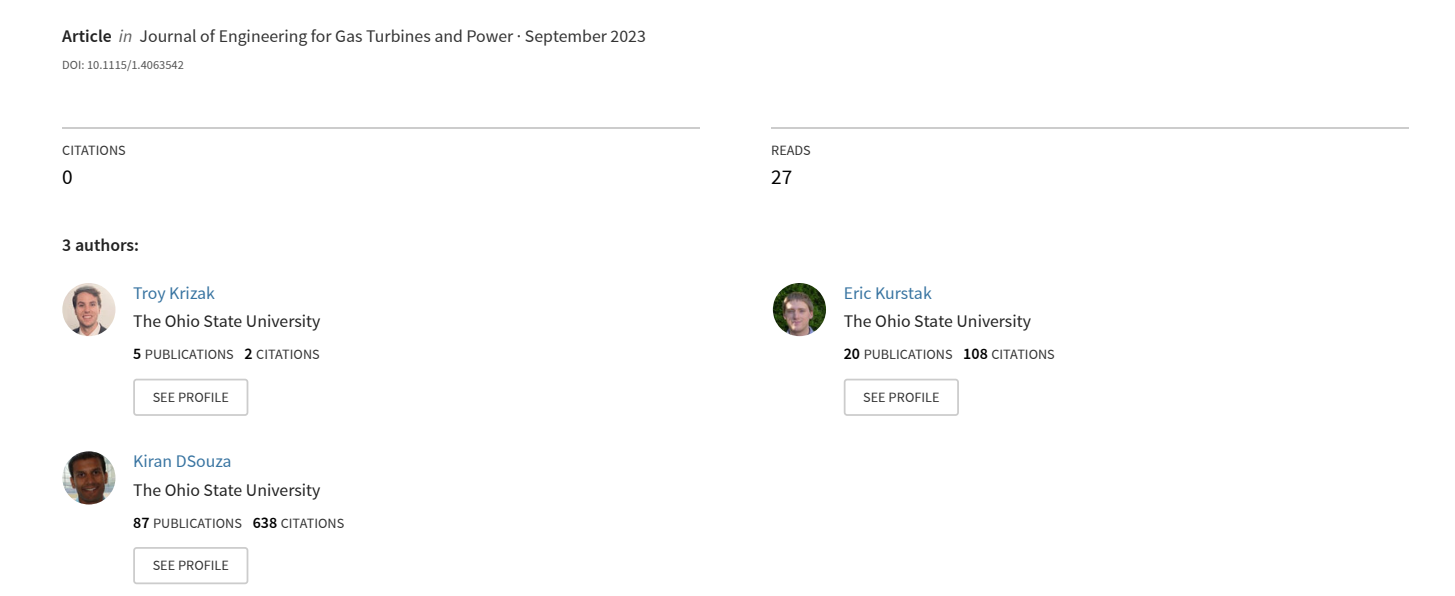
Damping and Stiffness Mistuning Effects in a Bladed Disk With Varied Disk Coupling



Damping and Stiffness Mistuning Effects in a Bladed Disk with Varied Disk Coupling

Troy Krizak

Gas Turbine Laboratory
Department of Mechanical
and Aeronautical Engineering
The Ohio State University
Columbus, OH 43235
Email: krizak.1@osu.edu

Eric Kurstak

Gas Turbine Laboratory
Department of Mechanical
and Aeronautical Engineering
The Ohio State University
Columbus, OH 43235
Email: eric.kurstak@gmail.com

Kiran D'Souza*

Gas Turbine Laboratory
Department of Mechanical and
Aeronautical Engineering
The Ohio State University
Columbus, OH 43235
Email: dsouza.60@osu.edu

ABSTRACT

Component mode mistuning (CMM) is a well-known, well documented reduced order modeling technique that effectively models small variations in blade-to-blade stiffness for bladed disks. In practice, bladed disks always have variations, referred to as mistuning, and are a focus of a large amount of research. One element that is commonly ignored from small mistuning implementations is the variation within the bladeto-blade damping values. This work seeks to better understand the effects of damping mistuning by utilizing both structural and proportional damping formulations. This work builds from previous work that implemented structural damping mistuning reduced order models formulated based on CMM. A similar derivation was used to create reduced order models with a proportional damping formulation. The damping and stiffness mistuning values investigated in this study were derived using measured blade natural frequencies and damping ratios from high-speed rotating experiments on freestanding blades. The two separate damping formulations that are presented give very similar results, enabling the user to select their preferred method for a given application. A key parameter investigated in this work is the significance of blade-to-blade coupling. The blade-to-blade coupling study investigates how the level of coupling impacts damping mistuning effects versus applying average damping to the bladed disk model. Also, the interaction of stiffness and damping mistuning is studied. Monte Carlo simulations were carried out to determine the amplification factors, the ratio of mistuned blade responses to tuned blade responses, for various mistuning levels and patterns.

INTRODUCTION

Bladed disk systems will always have some blade-to-blade property variations, this is referred to as mistuning. Mistuned systems are very important to study because the symmetry of the system is broken and can lead to vibration

^{*}Address all correspondence to this author.

localization and high amplitudes, which can lead to high cycle fatigue problems. Currently, there is a significant amount of work that has been done to capture stiffness mistuning, or variations in the natural frequencies of the blades, in the turbomachinery industry. Damping mistuning has been less of a focus but is still considered an important property to study. It is expected that each blade has its own individual damping value, similar to stiffness. Full finite element (FE) models can be used to study these mistuning characteristics, but for industrial FE models, reduced order models (ROMs) are vital to save on computation time and costs. A requirement for effective ROMs of industrial bladed disks is that they are generated from single sector models using cyclic analysis calculations, this is because the size of the full model is often too large for analysis.

Many ROMS have been developed to capture mistuning and its effects in turbomachinery. Small stiffness mistuning, in this work, is captured using a method called component mode mistuning (CMM) [1,2]. A similar method for small frequency mistuning is the fundamental mode of mistuning (FMM) method [3]. FMM is limited to single isolated blade dominated mode families, while CMM is more flexible and can handle multiple mode families and all types of modes if the model is large enough. One thing to note is that for small mistuning, CMM assumes that there is no change in mode shape of the blades, only a small frequency shift. After these models for small stiffness mistuning were developed, a number of other methods were developed to handle other types of mistuning including small geometric mistuning [4–6] and large mistuning [7]. Additionally, the challenge of multiple stages with different number of sectors combined with small mistuning [8,9], large mistuning [10,11], and aeroelastic effects [12] has been addressed. These ROM methods have also been used to model friction damping when underplatform dampers [13,14] and ring dampers [15,16] are installed on the bladed disk. Previously, a ROM was derived that implements structural damping variability within a single stage blisk [17]. This method is able to capture large variability in damping values as well as small stiffness mistuning. While this is a valid and useful method, a separate ROM that implements proportional damping was derived in this work. These two methods should align very well in trends and amplitude and give confidence in the other studies performed with the ROMs.

The primary goal of this study was to determine the impacts that damping mistuning has when coupled with stiffness mistuning. Changes in damping will directly impact the amplitudes of tip deflections of the blades. One way to determine if damping mistuning must be considered is running a ROM that uses both damping and stiffness mistuning to solve for an amplification factor, or a ratio between the mistuned blade and a perfectly tuned blade. The amplification factors for the ROMs are found using a harmonic analysis, which makes implementing the two types of damping straightforward. It is easy to reason that as the damping of the system is increased, blade deflections will decrease. More interesting will be to determine if the damping and stiffness mistuning have a coupled effect on the dynamics of the system. This work will include a Monte Carlo statistical analysis that lowers the effects of a specific mistuning pattern and gives a better idea about the general effects of mistuning on the bladed disk. Several cases were also ran where there is an outlier blade that will show if damping mistuning is only important for these specific cases, or if it must be considered for all mistuning patterns. Another point of interest was to determine how the coupling of the disk sectors impacts the damping mistuning effects. This disk coupling analysis is vital for dynamic design practices because there is an interest, especially in the aerospace industry, in making lightweight less stiff bladed disks and blisks. It is important to study the relationship between disk coupling and mistuning to determine the types of mistuning that may become even more important in these new designs.

In the following sections of this work, the ROMs for both structural and proportional damping will be derived and implemented. This will include a description of the modeling approaches with ANSYS and the creation of the ROM. Next, results of the damping mistuning studies are presented. Finally, some conclusions will be drawn from the results of these studies.

ROM DERIVATION

In this section, the derivation of the ROM that implements proportional damping is presented. The final equation of motion for the previously derived structural damping formulation is also included. These ROMs capture the effects of both damping and small stiffness mistuning. The derivation method for the proportional damping follows the same technique shown previously to find the structural damping ROM formulation [17]. After the derivation, the final equation of motion is compared to the ROM that utilizes structural damping. The full equation of motion for a standard dynamic system with damping is given in Eqn. (1). This equation includes the mass matrix, \mathbf{M} , damping matrix, \mathbf{C} , and the stiffness matrix, \mathbf{K} . $\mathbf{F}_{Applied}(t)$ is the applied time dependent forcing, which is a harmonic forcing in this

study.

$$\mathbf{M}\ddot{x} + \mathbf{C}\dot{x} + \mathbf{K}x = \mathbf{F}_{Applied}(t) \tag{1}$$

The equation of motion, when a modal reduction and Laplace transform is performed, can be seen in Eqn. (2). This modal reduction is important because it reduces the size of the dynamic system and makes solving equations of motion much faster and computationally less expensive. A selection of tuned normal mode shapes, Φ , can be used to reduce the forcing vector and the mass, damping, and stiffness matrices. Using a Laplace transform and implementing $s=i\omega$ gives the equation seen in Eqn. (2) where ω is the rotational forcing frequency. The vector p contains the modal coordinates of the system.

$$-\omega^{2} \mathbf{I} p + i\omega \Phi^{T} \mathbf{C} \Phi p + \Phi^{T} \mathbf{K} \Phi p = \Phi^{T} \mathbf{F}_{Applied}(i\omega)$$
(2)

The forcing is premultiplied by the mode shape matrix and can be denoted as f as seen in Eqn. (3).

$$f = \Phi^T \mathbf{F}_{Applied}(i\omega) \tag{3}$$

The stiffness matrix, using the modal reduction, can be reduced to a diagonal matrix of the tuned truncated eigenvalues, Λ^S , plus the variation in stiffness eigenvalues from the cantilever blade nominal stiffness, $\lambda_{CB,n}^{\delta}$ times the modal participation factors q_n . This reduction to the stiffness matrix can be seen in Eqn. (4).

$$\Phi^T \mathbf{K} \Phi = \mathbf{K}_{sys} = \Lambda^S + \sum_{n=1}^N q_n^T \lambda_{CB,n}^{\delta} q_n$$
(4)

Now one can utilize a linear approximation for the damping in the system. As previously stated, the linear approximation for proportional damping, β , was chosen to be implemented in this derivation. This proportional damping is simply a scalar applied to the stiffness matrix of the dynamic system. The approximated damping, including small variations in blade-to-blade proportional damping, β_n^{δ} , can be seen in Eqn. (5).

$$\Phi^T \mathbf{C} \Phi = \sum_{n=1}^N \beta_n \mathbf{K}_{sys} = \sum_{n=1}^N (\beta_{avg} + \beta_n^{\delta}) \mathbf{K}_{sys}$$
 (5)

Combining Eqn. (4) and Eqn. (5) and performing a modal reduction using the normal modes, the final damping matrix that includes both stiffness and proportional damping mistuning can be derived. This damping matrix reduction can be seen in Eqn. (6). Λ_n^{δ} is the diagonal matrix containing the blade to blade variations in eigenvalues.

$$\Phi^T \mathbf{C} \Phi = \sum_{n=1}^N (\beta_{avg} + \beta_n^{\delta}) (\Lambda^S + \Lambda_n^{\delta})$$
 (6)

One can now substitute the final reduced damping matrix from Eqn. (6) and the reduced stiffness matrix from Eqn. (4) back into Eqn. (2).

$$\left[-\omega^{2}\mathbf{I} + i\omega\left[\sum_{n=1}^{N}\beta_{avg}(\mathbf{K}_{sys}) + \sum_{n=1}^{N}\beta_{n}^{\delta}(\mathbf{K}_{sys})\right] + \mathbf{K}_{sys}\right]p = f$$
(7)

The final equation of motion that includes both proportional damping and stiffness mistuning can be seen in Eqn. (8). Where C^{δ} , given in Eqn. (9), is the damping mistuning matrix that includes factors from both damping and stiffness mistuning. δ_n is the variation of the stiffness in the n^{th} blade from the average stiffness of all the blades.

$$[-\omega^2 \mathbf{I} + (1 + i\omega \beta_{avq}) \mathbf{K}_{sys} + (i\omega) \mathbf{C}^{\delta}] p = f$$
(8)

$$\mathbf{C}^{\delta} = \sum_{n=1}^{N} q_n^T \beta_n^{\delta} (1 + \delta_n) \Lambda_{CB,n}^S q_n \tag{9}$$

The equation of motion for the proportional damping approximation can now be compared to the previously derived structural damping formulation. The equation of motion including structural damping can be seen in Eqn. (10) where the matrix for damping mistuning, C^{δ} , is given in Eqn. (11). The equation of motion is shown in a slightly different format than in [17] to make it easy to compare the proportional and structural damping formulations.

$$[-\omega^{2}\mathbf{I} + (1 + i\gamma_{avg})\mathbf{K}_{sys} + (i)\mathbf{C}^{\delta}]p = f$$
(10)

$$\mathbf{C}^{\delta} = \sum_{n=1}^{N} q_n^T \gamma_n^{\delta} (1 + \delta_n) \Lambda_{CB,n}^S q_n \tag{11}$$

MODELING APPROACH

This section outlines the modeling approach used to test the effect of damping and stiffness mistuning on the bladed disk system. In particular, a harmonic analysis was used to find maximum tip deflection amplitudes of the bladed disk for a number of tuned and mistuned system realizations and levels of mistuning.

In order to compare the various numerical test cases, an amplification factor metric, or the ratio between the tuned and mistuned systems was calculated. This amplification factor is the maximum amplitude of the mistuned system divided by the maximum amplitude of the tuned system. The amplification factor was calculated by running a harmonic analysis for both the tuned and mistuned cases, finding the maximum tip deflection, and then finding the ratio between the responses. This metric can be used for the maximum of the overall system or for the maximum response of individual blades. The amplification factor gives a good understanding of the impact of damping and stiffness mistuning because it is a direct comparison between the tuned and mistuned cases. One can also find the amplification factors of any damping and stiffness mistuning scale combination. While amplification factors for the overall system are always greater than one, individual blades can have amplification factors less than one.

This work studies an industrial bladed disk, with a complex geometry, requiring a large FE model. This bladed disk has been studied extensively both experimentally [18–21] and computationally [22, 23]. A single sector model and cyclic analysis needed to be used to generate the ROM due to the computational size of the model. The cyclic

symmetry boundary conditions were applied to the high and low faces of the disk. Since the focus of this work is on linear damping models, the freestanding model with no underplatform dampers is the focus of this analysis. The mass and stiffness matrices can be found by using a static analysis, followed by a prestressed modal analysis to solve for the normal modes of the blades at a desired speed. Similarly, the cantilever blade modes were found in the same fashion but with the disk nodes held fixed. During the prestressed modal analysis, the up and down stream disk interface nodes were fully constrained to simulate where the bladed disk is fixed. The disk stiffness was tuned previously to match forced rotating test results and have been previously shown to be accurate [18,20]. All tip deflections were measured at a single node at the tip of the blade for all cases. Figure 1 shows the results of a harmonic analysis for a single blade and for all the blades of the system, with a random stiffness and damping mistuning pattern applied. Both the tuned blade and the mistuned blade responses can be observed. From this harmonic analysis, the amplification factor can be solved by finding the ratio of the maximum blade amplitudes to the tuned response. The variation in maximum amplitudes for each blade of the mistuned system is clearly seen in Fig. 1(b), which leads to different amplification factors for each blade (some less and some greater than one). Note that the amplification factor for the overall system is the ratio of the maximum responding blade of all the mistuned blades divided by the tuned response.

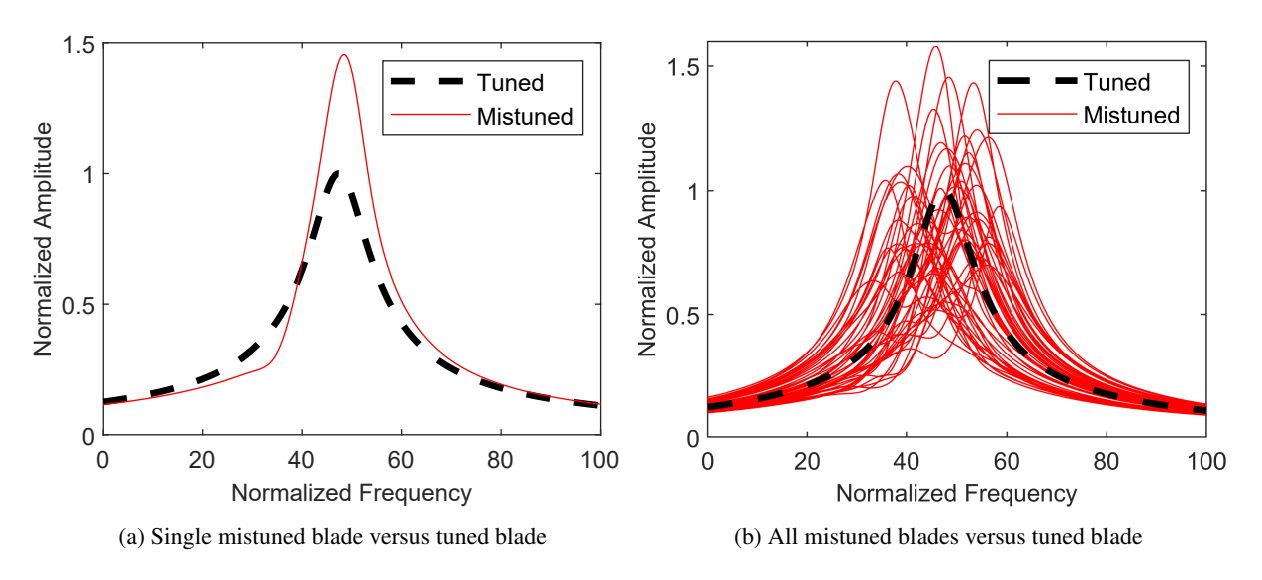


Fig. 1: Sample results of a harmonic analysis

Since two different damping formulations were used in this work, the applied damping values need to be equivalent if comparisons are going to be made. The original damping and stiffness mistuning patterns were calculated using tip timing data from rotating experiments, and the damping for each blade was reported as a damping ratio, ζ . Due to the proprietary nature of this work, the baseline damping ratio cannot be given, so only mistuning values are presented. In the experiments, air jets were used to force synchronous vibrations while the bladed disk was accelerated through critical speeds. These rotating experiments studied the first bending mode, so it will be the focus of the ROMs in this work. Tip deflections were measured using optical laser light probes, and damping ratios were extracted for each blade using the half-power bandwidth method. The tip timing system also measured the stiffness mistuning pattern by extracting the frequencies at the maximum blade amplitudes. Damping ratios can be converted to a γ value for structural damping, or a β value for proportional damping. The equations for solving for β and γ are given in Eqn. (12) and Eqn. (13), respectively, where ω_n is the average natural frequency of all of the blades in a test run. The damping values that are measured in the experiments are assumed to be solely interior material damping with no friction effects from the blade and disk contacts. This has been shown in previous work to be a valid assumption for a single rotational speed.

$$\beta = \frac{2\zeta}{\omega_n} \tag{12}$$

$$\gamma = 2\zeta \tag{13}$$

In order to simulate different levels of mistuning, a scaling factor can be applied that either increases or decreases the amount of damping or stiffness mistuning. This scaling factor is applied to the original mistuning pattern and then damping values can be converted into structural or proportional damping values. Figure 2 shows the mistuning scale being applied to a mistuning pattern for the original mistuning pattern, a double scale, and a half scale. Care must be taken when applying the scaling to both the stiffness and damping mistuning. CMM assumes that the levels of stiffness mistuning are small and will contain a large amount of error if the mistuning values increase over a certain threshold. The scaling of the damping mistuning must also be carefully adjusted, this is because the amplitudes of the blade will trend towards infinity if damping gets close to zero. To avoid these complications with the stiffness and damping mistuning, the scales of the mistuning were chosen to not break these assumptions to keep results realistic. Initial checks were ran to determine the scaling that can be applied to the system.

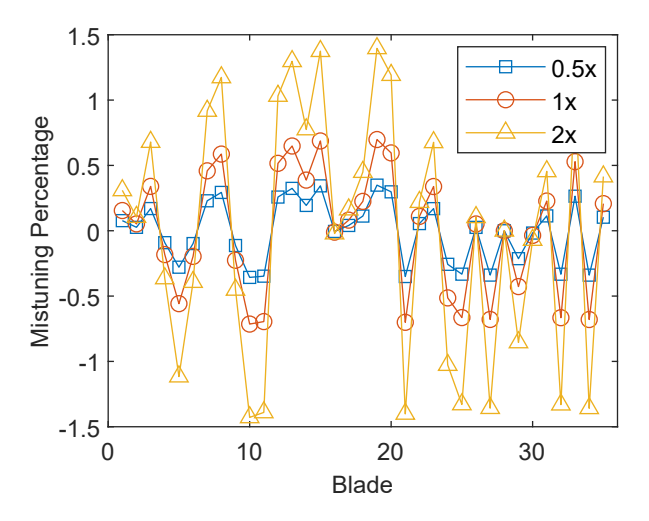


Fig. 2: Examples of scaling applied to mistuning pattern

For some of the analyses, a Monte Carlo statistical analysis was used to lower the impact that a specific mistuning pattern has on the conclusions about how mistuning impacts the dynamics of the system. The different mistuning patterns were generated randomly to have similar statistical properties as the experimentally measured mistuning patterns [18, 20]. As mentioned previously, mistuning patterns were measured during experimental testing of an actual bladed disk and the standard deviation and average values were used to generate new mistuning patterns with the same properties (average and standard deviation). These different mistuning patterns were also scaled to different levels to show the impact in the amount of mistuning. One hundred different mistuning patterns were generated for both the damping and stiffness mistuning, and then scaled to get different levels of mistuning. It is important to do this scaling instead of creating new patterns for each level to have consistency between the different mistuning scale cases. Monte Carlo analysis is used to understand how random mistuning effects the system dynamics and not focus on the results of a single mistuning realization.

RESULTS

With the damping mistuning ROMs and modeling methods discussed, analyses determining the effect of damping and stiffness mistuning are presented. The first analysis shows that the proportional and structural damping ROM methods are similar as one would expect based on the similarities in the linear damping approximations. Next, the overall effects of the damping and stiffness mistuning are analyzed to show how damping mistuning can have an impact on the system. After, the disk stiffness is varied to determine the impact of the coupling between blades on the relationship of damping and stiffness mistuning. Finally, there is an analysis where the damping values of all the blades are the same except one that has half the amount of damping. This analysis shows the effect that an outlier blade has on the neighboring blades and the effect on the overall system. As mentioned, the amplification factor will be used as a metric for all of the analyses. The responses for all of the studies in this work were computed from a harmonic analysis where the system was excited by an engine order six excitation. As in the experiments, the first bending mode family is the focus of these modeling studies.

Comparison of Damping Mistuning ROMs

The first analysis performed in this work is a comparison between the linear structural and proportional damping ROMs. This comparison is important because it ensures that the two ROMs are in good agreement as one would expect. Figure 3 compares the overall system amplification factor for 100 different damping and stiffness mistuning patterns at different mistuning levels for damping and stiffness for both the structural and proportional damping models. Note that at zero damping and stiffness mistuning, the system is tuned and therefore the amplification factor is precisely one for both damping formulations, as expected. Also, note that the mistuning level in the physical experimental system corresponds to the case where the damping and stiffness mistuning scaling is equal to one. Values less than one correspond to mistuning levels that were lower than those measured in the experiments and values greater than one correspond to mistuning levels greater than those measured in the experiments. Figure 3 clearly shows the effects of scaling the damping and stiffness mistuning and their interaction. It should be noted that the two mistuning sources tend to amplify each other such that having both sources of mistuning leads to greater amplification factors than either one individually. Moreover, it can be observed that the amplification factor tends to continue to increase with increasing damping mistuning levels whereas the amplification factor tends to plateau for increasing stiffness mistuning only after a scaling of about two. It can also be seen that both the trends and the amplitudes of the amplification factors from the approximated damping formulations line up well.

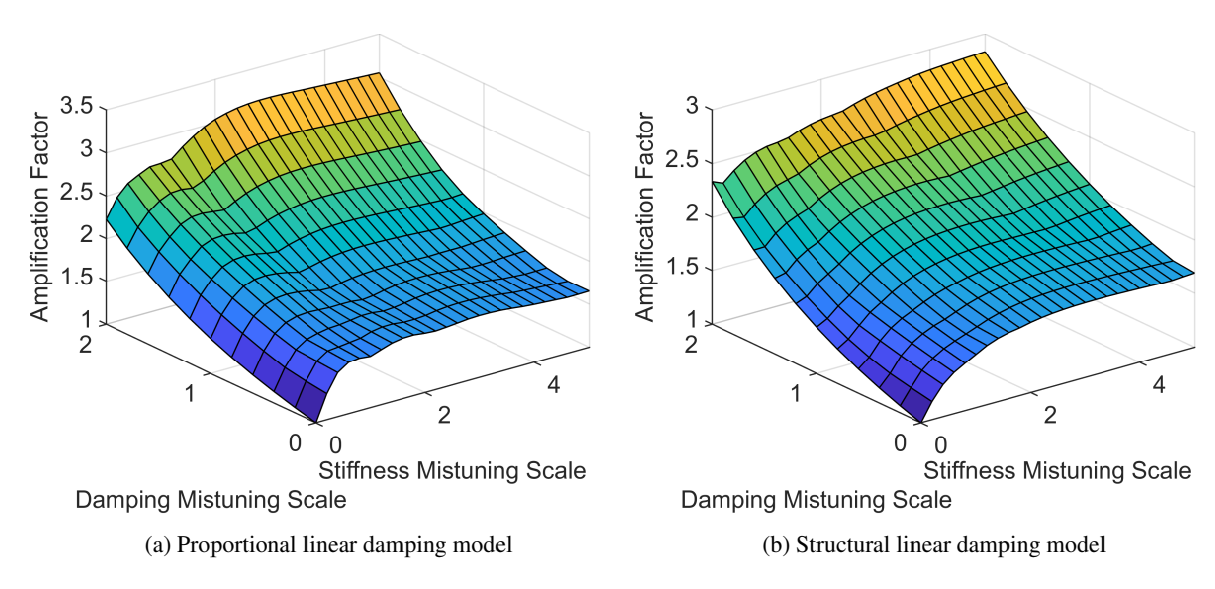
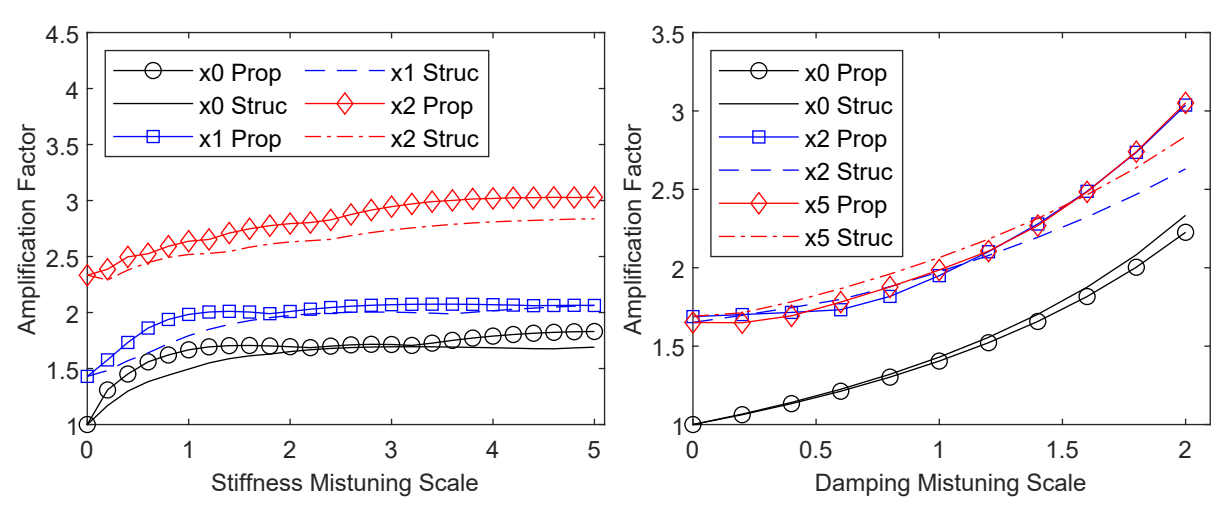


Fig. 3: Amplification factor plots for damping and stiffness mistuning comparing two linear damping formulations

Figure 4 shows a comparison of the two damping formulations at different mistuning levels. For Fig. 4(a), the three lines represent different damping mistuning levels (0, 1, and 2) while the stiffness mistuning level varies from 0 to 5. Similarly, for Fig. 4(b), the three lines represent different stiffness mistuning levels (0, 2, and 5) while the damping mistuning level varies from 0 to 2. Figure 4 again shows that the structural and proportional damping mistuning ROMs are in good agreement. While there are small differences in the amplitudes of the amplification factors, this is not unexpected, the trends are very similar between the two damping formulations. With the two damping formulations shown to provide similar results, the remainder of the work will contain results with proportional damping mistuning only.



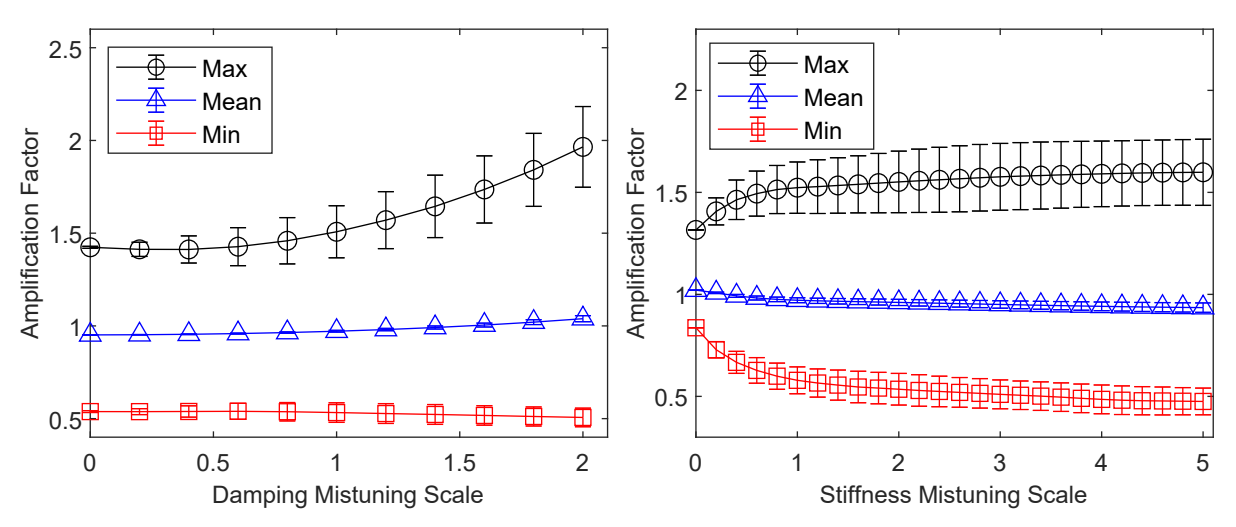
(a) Effect of stiffness mistuning on 3 damping mistuning levels (b) Effect of damping mistuning on 3 stiffness mistuning levels

Fig. 4: Comparison of three individual mistuning patterns for varying stiffness mistuning levels and damping mistuning levels

Effects of Damping Mistuning

The next analysis performed was to determine the overall effect that damping mistuning has on the bladed disk. This analysis is important because it will determine the dynamic effects of the damping and stiffness mistuning, which will provide insight into the necessity of including damping mistuning in the modeling of bladed disk systems if it is expected to be present. If there is little to no impact from damping mistuning, then the extra complexity from adding it can be avoided. The Monte Carlo analysis was utilized for this study. The amplification factor results from this study can be seen in Fig. 5. In Fig. 5(a), the damping mistuning scale is increased for a single stiffness mistuning pattern (with 100 damping mistuning patterns at each mistuning level), and in Fig. 5(b) the stiffness mistuning scale is increased for a single damping mistuning pattern (with 100 stiffness mistuning patterns at each mistuning level). For each of the mistuning patterns at each level, values are found for the maximum, mean, and minimum amplification factors for the blades. Then, an average value and standard deviation can be found for the three cases. The marker indicates the average values, and the error bars denote the standard deviation across the different mistuning patterns.

As seen in both plots in Fig. 5, there is an impact on both the average values and standard deviations of the amplification factors with the scaling of both the damping and stiffness mistuning. In Fig. 5(a) it can be seen that as damping mistuning scale increases, the amplification factor average and standard deviation increases for the maximum values of the blades. For both the mean and the minimum values, however, the amplification factors stay very consistent over the increasing damping mistuning level. This makes sense because even when the mistuning scale increases, the mean value of the damping stays the same. This shows that, for this specific bladed disk, the damping mistuning has a significant impact on the maximum blade amplitudes and a minimal impact on the mean and minimum deflection values.



(a) Single stiffness mistuning pattern and 100 different damp- (b) Single damping mistuning pattern and 100 different stiffing mistuning patterns

ness mistuning patterns

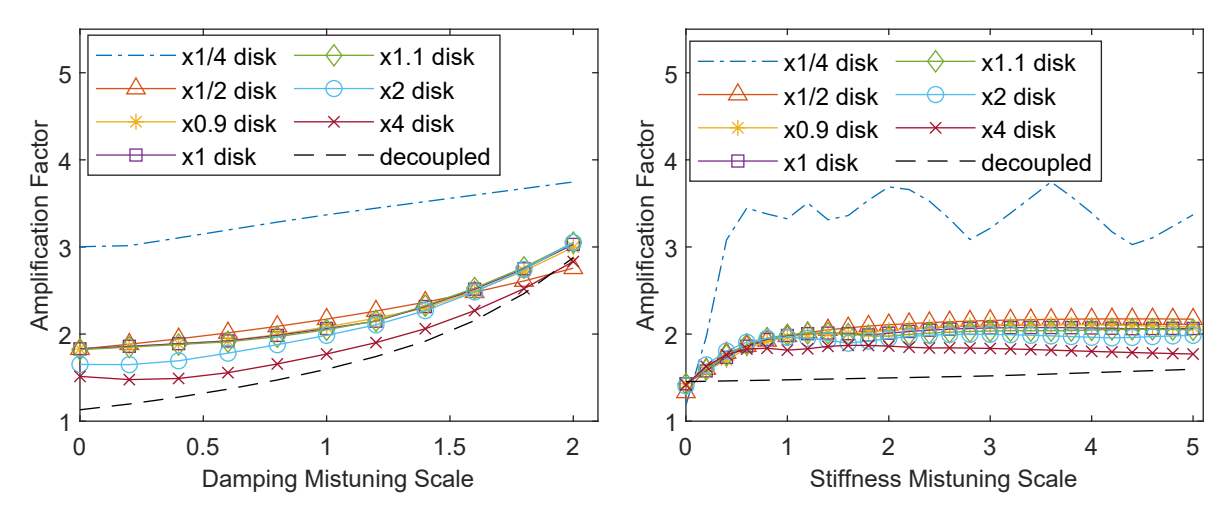
Fig. 5: Interaction between damping and stiffness mistuning

In Fig. 5(b) it can be seen that the maximum values increase and the minimum values decrease with the average values staying the same for the increase in stiffness mistuning. This shows that stiffness mistuning, for a single damping mistuning pattern, will have a significant impact on the dynamics of this bladed disk system. Stiffness mistuning has been previously studied and this result is in line with previous literature. When comparing the two plots, it can be seen that values for the increasing damping mistuning amplification factors are much higher and trending towards being higher for the maximum case. The amplification factors for the average maximum values of the stiffness mistuning seems to peak at a little over 1.5 whereas for the damping mistuning it continues to increase to about two as the mistuning scale is increased. The minimum and average values are not too dissimilar between the two cases, it should be noted that the maximum value is typically of greatest importance since that is what affects the fatigue life. These results show the importance of damping mistuning and its interaction with stiffness mistuning and the importance in modeling both when there are significant levels of mistuning.

Disk Stiffness/Coupling Analysis

The next analysis performed studies the impact of disk stiffness on the amplification factors of a bladed disk with damping and stiffness mistuning. This change in disk stiffness affects the coupling between the blades through the disk. For this study, amplification factors were solved for FE models that vary in disk stiffness. As the stiffness of the disk increases, the blades will be more and more decoupled. This analysis is important because different bladed disks and blisks will have different stiffness values for the disk portion of the system. This will mean that if there is an impact from the damping mistuning, some bladed disk manufacturers will be more concerned when designing bladed disks. For example, the aerospace industry is always trying to reduce the size and weight of bladed disks and blisks, which can lead to a decreased stiffness in the disk designs. This means that the aerospace manufacturers may need to be more concerned when it comes to the coupling of damping and stiffness mistuning with their less stiff disks. The amplification factors results from this study can be seen in Fig. 6. The different cases show where the disks are a fourth, half, 90 percent, 110 percent, double, and four times the original FE disk stiffness. A case where the disk sections are fully decoupled is also analyzed. This is when all the nodes in the disk are fixed, which isolates each blade from all others. This study was performed with increasing stiffness and damping mistuning with a single mistuning pattern of the other parameter.

Figure 6 shows how the disk stiffness can have a direct impact on amplification factors with increasing mistuning scales. Figure 6(a) shows that as the disk stiffness decreases, generally the amplification factors increase. Also, as the damping mistuning scale is increased, the amplification factors increase. This shows that with a less stiff disk, there



(a) Amplification factor for 100 different damping mistuning (b) Amplification factor for 100 different stiffness mistuning patterns with a single stiffness mistuning pattern patterns with a single damping mistuning pattern

Fig. 6: Interaction between disk stiffness and mistuning

needs to be more care when it comes to modeling the dynamics of the bladed disk and damping mistuning can become more important. Figure 6(b) also shows that the amplification factors decrease when the disk stiffness is increased. In both the damping and stiffness mistuning cases, the fully decoupled disk gives a lower bound for the amplification factors of the system. This can be helpful to find the lower limit to show how a fully decoupled system will react. Both plots also show that there is not much change when it comes to small variations in disk stiffness. This means that there is less concern when there is small variation in disk stiffness, however, large changes in disk stiffness can have a significant impact.

Outlier Analysis

Lastly, a study was performed where a single blade is chosen to be an outlier to understand how disk stiffness and mistuning level will impact this outlier blade. All blades in the system have the same damping value and the outlier will have a value half that of the rest of the blades. This provides insight to how the individual blade reacts to changing amounts of damping and stiffness mistuning. Again, a change in the disk stiffness is applied to determine the effect of the outlier with a varying amount of disk stiffness. This is important because it tells the relationship of the blade with the surrounding blades. The scaling of the damping mistuning again does not affect the overall average damping of the system but will only affect the damping mistuning values of the blades. This means that the non-outlier blades of the system are slightly affected by the damping mistuning scale increasing, but much less than that of the outlier. The analysis was performed with a tuned stiffness and a single unscaled stiffness mistuning pattern applied, while the damping mistuning was varied. The maximum mistuning scale is less than that of previous studies in this work to prevent the outlier damping from reaching zero. The results for the impact of damping mistuning on the outlier blade are given in Fig. 7. When the damping mistuning scale is equal to one, the outlier blade's damping value is equal to half that of the other blades. As the damping mistuning scale is then increased, the outlier blade becomes even more separated from the other blades damping values.

The amplification factors for both the tuned and mistuned stiffness are directly impacted by the level of disk stiffness. This makes sense because as the disk stiffness is increased, the blades will become more and more decoupled. This will affect how much damping the neighboring blades will have on the outlier blade. It can also be noted that the amplification factor rises as the damping mistuning scale increases. This makes sense because as the scale increases, the outlier blade damping decreases. The fully decoupled outlier blade gives an upper bound of the amplification factors.

In addition to observing the outlier blade in this analysis, the amplification factors of the neighboring blades to

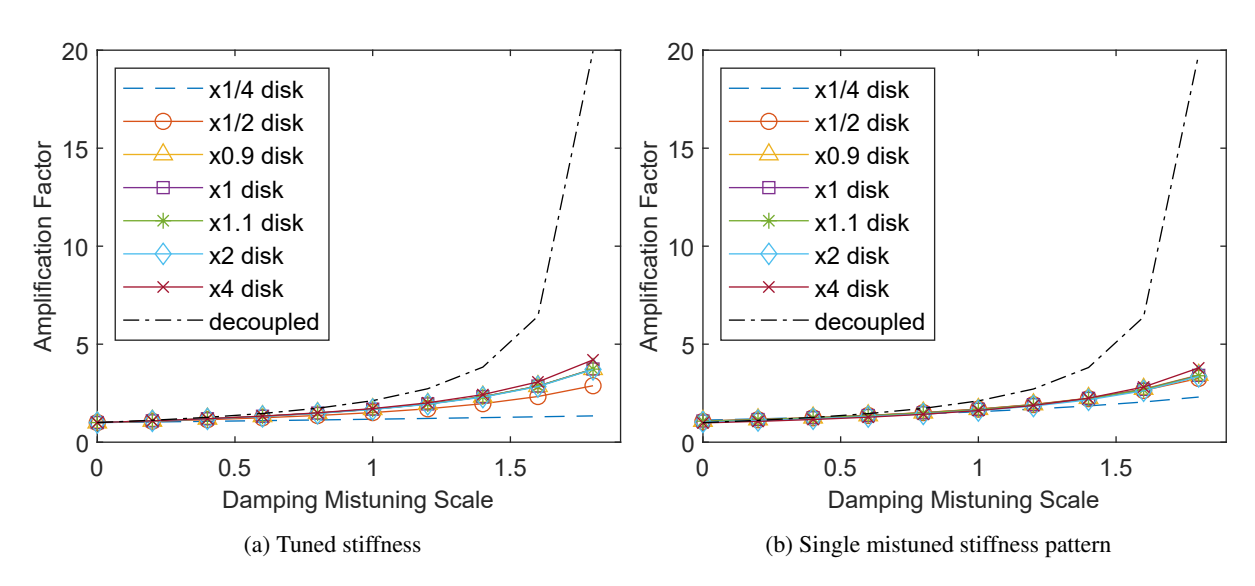


Fig. 7: Effect of damping mistuning and disk stiffness on outlier blade

the outlier were extracted. The two neighboring blades that are the focus of this study are the two blades that are on each side of the outlier blade. The results for the neighbors for the tuned and mistuned cases can be seen in Fig. 8 and Fig. 9, respectively.

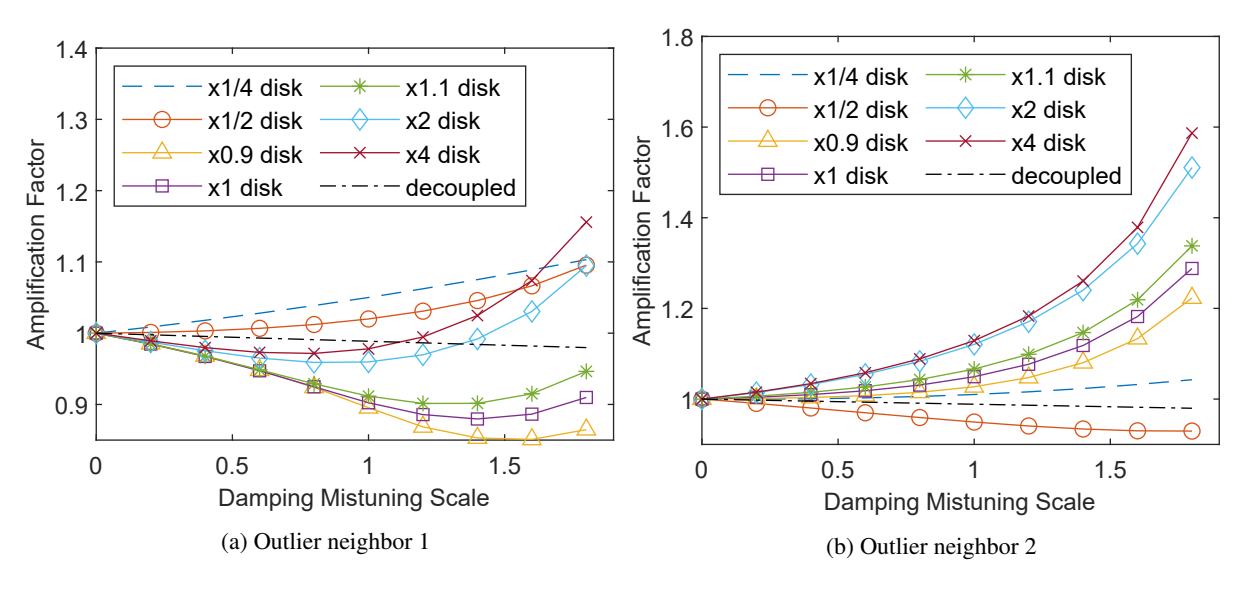


Fig. 8: Effect of damping mistuning on neighbors of outlier blade for tuned stiffness case

Again, the disk stiffness has a direct impact on the amplification factors because as the disk gets more decoupled, there is less of an effect from the outlier on the neighboring blades. The neighbors, however, have a much more complicated response than the outlier blade, especially when stiffness mistuning is present. The neighbors no longer see a monotonic rise in amplification factors as disk stiffness is increased. This shows that there are complicated interactions between the outlier and the neighboring blades and is very hard to predict. It can also be seen that the two neighboring blades will be affected differently by the outlier blade. This again means that the interaction between

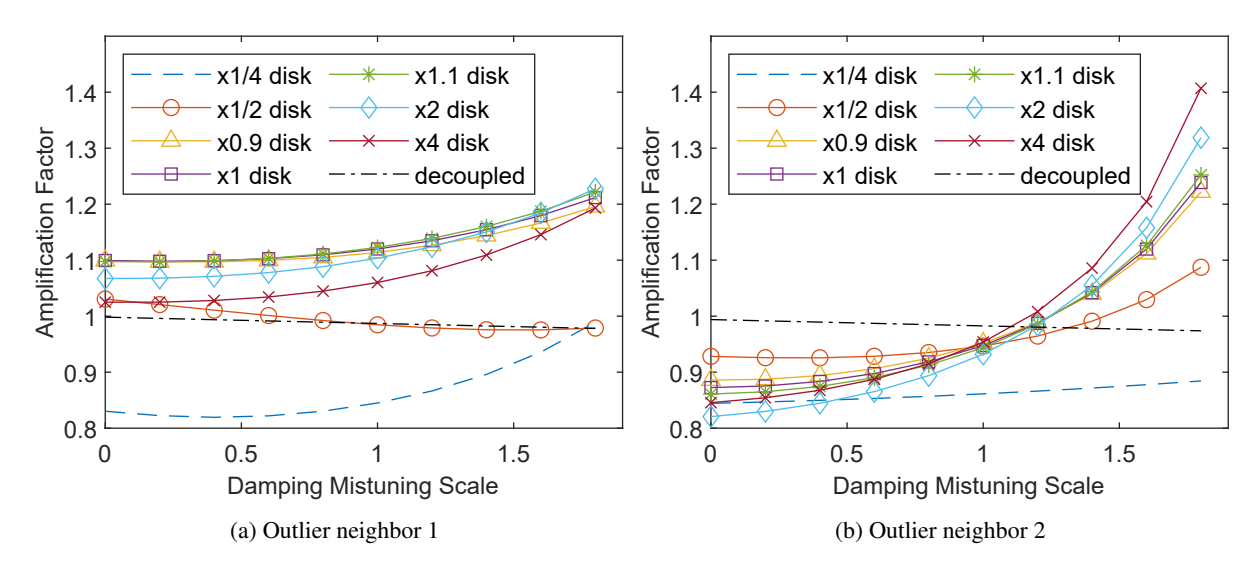


Fig. 9: Effect of damping mistuning on neighbors of outlier blade with stiffness mistuning applied

the blades is complicated and hard to predict. For the neighbors, the decoupled system no longer is a bound for the amplification factors and now is dependent on the values for the damping and stiffness of the neighboring blades.

CONCLUSIONS AND DISCUSSON

This work focused on investigating interactions of damping and stiffness mistuning on reduced order models (ROMs) of an industrial bladed disk with realistic mistuning properties extracted from rotating experiments. These ROMs are built and reduced utilizing a variation of the component mode mistuning method to implement the mistuning. This work derived the expressions for implementing a proportional damping mistuning model and the results were compared with a previously developed structural damping mistuning model. The methods were shown to have similar results so that both formulations would lead to similar conclusions, and proportional damping mistuning was used for the remainder of the analysis.

One of the primary conclusions from this work is that damping mistuning can have a large effect on the expected amplification factor of the response. Moreover, when coupled with the stiffness mistuning, results in a higher amplification factor than either individual mistuning mechanism on its own. Unlike stiffness mistuning, the effects of the damping mistuning did not tend to drop off as the mistuning increased and continued to increase as the damping mistuning increases. This leads to the need to carefully consider damping mistuning in the design, modeling, and testing of new bladed disk designs.

Another conclusion, which was previously known for stiffness mistuning, is that the coupling between blades through the disk stiffness greatly impacts the damping mistuning effects. Irrespective of the level of coupling between blades, when the damping mistuning increases the amplification factor increases. This is in contrast to stiffness mistuning, which can actually remain flat or even decrease as the mistuning level increases and is dependent on the blade-to-blade coupling. Also, in agreement between the damping and stiffness mistuning is that the greater the blade to blade coupling through a less stiff disk the higher the amplification factor tended to be.

Finally, it can be concluded that if there is an outlier blade with much less damping than the other blades it can have a dramatic effect on the amplification factors. This is true whether the system has a tuned or mistuned stiffness. In this case the lower the coupling is between blades (higher disk stiffness), the greater the amplification factor results. Also, it should be noted that small changes in the disk stiffness did not generally have a large impact, but by reducing it by a factor of four or making it rigid is where the large changes were seen.

Future work in this research is determining a metric for quantifying the amount of coupling between blades. As previously discussed, the amount of coupling can be very important in determining how big an impact damping mistuning will have on the dynamics of the system.

ACKNOWLEDGEMENTS

The authors acknowledge the financial support of Siemens Energy Inc. in running experiments and the support of program manager Heinrich Stueer. Additionally, the analysis was supported by the US National Science Foundation under Grant No. 1902408 and program manager Dr. Harry Dankowicz. The authors gratefully acknowledge the support of the OSU GTL staff members and Dr. Randall Mathison in the setup and operation of the facility. Any opinions, findings, and conclusions or recommendations expressed in this paper are those of the authors and do not necessarily reflect the views of the National Science Foundation or Siemens Energy Inc.

REFERENCES

- [1] Bladh, R., Castanier, M. P., and Pierre, C., 2001. "Component-mode-based reduced order modeling techniques for mistuned bladed disks Part I: Theoretical models". *Journal of Engineering for Gas Turbines and Power Transactions of the ASME*, **123**(1), pp. 89–99.
- [2] Bladh, R., Castanier, M. P., and Pierre, C., 2001. "Component-mode-based reduced order modeling techniques for mistuned bladed disks Part II: Application". *Journal of Engineering for Gas Turbines and Power Transactions of the ASME*, **123**, pp. 100–108.
- [3] Feiner, D. M., and Griffin, J. H., 2004. "Mistuning identification of bladed disks using a fundamental mistuning model–part I: Theory". *Journal of Turbomachinery*, **126**(1), Mar., pp. 150–158.
- [4] Baek, S., and Epureanu, B. I., 2017. "Reduced-order models of blisks with small geometric mistuning". *J. Vib. Acoust.*, **139**(4), p. 041003.
- [5] Beck, J. A., Brown, J. M., Runyon, B., and Scott-Emuakpor, O. E., 2017. "Probabilistic study of integrally bladed rotor blends using geometric mistuning models". AIAA SciTech Forum. American Institute of Aeronautics and Astronautics.
- [6] Beck, J. A., Brown, J. M., Kaszynski, A. A., Carper, E. B., and Gillaugh, D. L., 2019. "Geometric Mistuning Reduced-Order Model Development Utilizing Bayesian Surrogate Models for Component Mode Calculations". *Journal of Engineering for Gas Turbines and Power*, 141(10), 09. 101013.
- [7] Madden A.; Epureanu, B. I.; Filippi, S., 2012. "Reduced-order modeling approach for blisks with large mass, stiffness, and geometric mistuning". *AIAA Journal*, **50**(2), Feb., pp. 366–74.
- [8] D'Souza, K., and Epureanu, B. I., 2011. "A statistical characterization of the effects of mistuning in multistage bladed disks". *Journal of Engineering for Gas Turbines and Power*, **134**(1), January, pp. 1–8.
- [9] Besem, F. M., Kielb, R. E., Galpin, P., Zori, L., and Key, N. L., 2016. "Mistuned Forced Response Predictions of an Embedded Rotor in a Multistage Compressor". *Journal of Turbomachinery*, **138**(6), JUN.
- [10] Kurstak, E., and D'Souza, K. X., 2017. "Multistage blisk and large mistuning modeling using fourier constraint modes and prime". *Journal of Engineering for Gas Turbines and Power*, Dec.
- [11] Kurstak, E., and D'Souza, K., 2020. "A Statistical Characterization of the Effects and Interactions of Small and Large Mistuning on Multistage Bladed Disks". *J. Eng. Gas Turbines Power*, **142**(4), Feb. 041015.
- [12] D'Souza, K., Jung, C., and Epureanu, B. I., 2013. "Analyzing mistuned multi-stage turbomachinery rotors with aerodynamic effects". *Journal of Fluids and Structures*, **42**, Oct., pp. 388–400.
- [13] Pesaresi, L., Salles, L., Jones, A., Green, J., and Schwingshackl, C., 2017. "Modelling the nonlinear behaviour of an underplatform damper test rig for turbine applications". *Mechanical Systems and Signal Processing*, **85**, pp. 662 679.
- [14] Zucca, S., Firrone, C. M., and Gola, M., 2013. "Modeling underplatform dampers for turbine blades: A refined approach in the frequency domain". *Journal of Vibration and Control*, **19**(7), May, pp. 1087–1102.
- [15] Laxalde, D., Thouverez, F., Sinou, J. J., and Lombard, J. P., 2007. "Qualitative analysis of forced response of blisks with friction ring dampers". *European Journal of Mechanics A/Solids*, **26**(4), pp. 676–687.
- [16] Laxalde, D., and Thouverez, F., 2007. "Non-linear vibrations of multi-stage bladed disks systems with friction ring dampers". In Proceedings of the ASME International Design Engineering Technical Conferences and Computers and Information in Engineering Conference 2007, Paper DETC2007-34473, ASME.
- [17] Anish G. S. Joshi, B. I. E., 2012. "Reduced Order Models for Blade-To-Blade Variability in Mistuned Blisks". *Journal of Vibrations and Acoustics*, **134**.
- [18] D'Souza, K., Kurstak, E., Ruff, K., and Dunn, M., 2020. "Development of an Experimental Facility for Conducting Blade Damping and Mistuning Studies at Design Speed". *AIAA Journal*, **58**(6).

- [19] Kurstak, E., and D'Souza, K., 2021. "An Experimental and Computational Investigation of a Pulsed Air-Jet Excitation System on a Rotating Bladed Disk". *Journal of Engineering for Gas Turbines and Power*, **143**(1).
- [20] Kurstak, E., and D'Souza, K., 2021. "Experimental Investigation of Bladed Disk Dynamics at Design Speed Under Synchronous Vibration". *AIAA Journal*, **59(10)**, pp. 4123–4133.
- [21] Krizak, T., Kurstak, E., and D'Souza, K., 2023. "Experimental and Computational Study of a Rotating Bladed Disk with Under-Platform Dampers". *AIAA Journal*.
- [22] Kurstak, E., and D'Souza, K., 2023. "Parametric Investigation of the Vibratory Responses of Reduced-Order Model Simulations of Rotating Bladed Disks". *AIAA Journal*.
- [23] Kurstak, E., Look, K., and D'Souza, K., 2020. "Mistuning Identification for Rotating Bladed Disks Using Stationary Measurements and Reduced Order Models". In Proceedings of the ASME International Design Engineering Technical Conferences, ASME.